PHYSICAL REVIEW B VOLUME 30, NUMBER 2 15 JULY 1984

Possibility of interpreting amorphicity as spatial chaos

P. Reichert and R. Schilling
Institut für Physik der Universität Basel, CH-4056 Basel, Switzerland
(Received 28 November 1983)

In order to gain insight into whether amorphicity can be interpreted as spatial chaos, we investigate one-dimensional chaotic configurations of atoms. These configurations are generated by the Baker transformation or, equivalently, by the Bernoulli shift, which is characteristic for chaos. We show that the distribution function G_j of the jth nearest-neighbor distances of these configurations is asymptotically (as $j \to \infty$) a Gaussian distribution with a width growing as $\sqrt{j}$ (local limit theorem). Furthermore, the pair distribution function G exhibits peaks related to the positions of nearby atoms, but in the limit of large distances these oscillations go to zero, and the pair distribution function converges to a constant, as expected for amorphous solids.

I. INTRODUCTION

Two different concepts have been developed to construct models of the atomic arrangement of amorphous structures. The oldest one, introduced to describe the structure of amorphous solids with covalent bonds, such as window glass (SiO_2) or amorphous semiconductors (Si, Ge), is the concept of random networks, originally due to Zachariasen.[1] The main idea of this approach is to build random structures in arranging the atoms in such a way that the lengths and angles of the bonds do not deviate much from their counterparts in the crystalline phase of the substance. The resulting structure is then topologically different from the crystal, but with preservation of the coordination number. Polk[2] and Polk and Boudreaux[3] used tetrahedrally coordinated random networks to simulate the atomic arrangement of armophous Si and Ge. The radial distribution function they obtained was in quite good agreement with the experimental one. Dandoloff, Döhler and Bilz[4,5] proposed a tetrahedrally coordinated random network with still more local order. It consists, apart from small distortions, only of two "unit cells," a 5- and 6-ring (but a different 6-ring than in diamond structure).

The other concept, developed to build models of metallic glasses, is dense random packing of hard spheres. This can be done according to geometrical or energetical conditions. The geometrical construction, which simulates vapor deposition onto a solid substrate, operates, according to Bennett,[6] as follows: Starting with a seed cluster one deposits additional spheres at the surface of the growing cluster. The site where to place the next sphere is chosen according to a global (minimal distance to the center of the seed cluster) or a local (minimal distance to the plane of the three nearest neighbors) criterion. The second, energetical method consists of spreading atoms randomly in space and relaxing them, according to a specified pair potential, into a minimum energy configuration (see e.g., Maeda and Takeuchi[7]). In both cases the resulting pair distribution function agrees very well with that of an amorphous solid: It exhibits more or less pronounced peaks, related to nearest, next-nearest neighbors, and so on, which disappear for growing distance.

There are also methods which are applicable to both covalent and metallic solids. One reason for this is the possibility of associating unambiguously a random network with an arbitrary configuration,[8] especially with one generated by dense random packing. Such random networks do not generally fulfill the above-mentioned characteristics of small distortions of bonds, and therefore do not necessarily correspond to covalent structures. An example of such a concept, which is applicable to both types of solids, is the gauge theory of amorphous structures by Rivier and Duffy,[9,10] which explains in a natural way the existence of two-level systems, which seem to be characteristic for glasses. This approach shows impressively the power of topological arguments. Another interesting construction is due to Kléman and Sadoc.[11,12] It is based on the idea that local arrangements of atoms, which cannot fill Euclidean space regularly, may do this in curved space. The amorphous structure is then obtained by mapping the regular structure within the curved space into Euclidean space. The patching of such local mappings induces two types of effects: distortions, which keep local order in the interior of the image of one patch, and defects in local order at the boundaries.

In this paper we follow a quite different approach, which can be characterized by the following question: *Can amorphous structures be interpreted as spatial chaos?* By the notion "spatial chaos" we mean a spatial analogy to irregular time evolution, which has been discovered in dynamical systems.[13–15] The possibility of such a connection between spatial chaos, obtained from dynamical systems and amorphicity, was probably first mentioned by Aubry.[16] Another approach to spatial chaos is due to Ruelle,[17] who proposed the existence of "turbulent crystals" as thermodynamic equilibrium states at nonzero temperature.

In order to find an answer to the question raised above, we restrict our considerations, as a first step, to one-dimensional models, which lead to chaotic stationary configurations. The restriction to one-dimensional systems, although making a comparison with real systems in nature difficult, also allows us to investigate the question of how far topological defects (which are absent in one dimension) are important for amorphous structures.

Such one-dimensional models for a classical chain of interacting atoms have been studied by several authors; in particular, Aubry[18] and Janssen and Tjon[19] have shown under certain conditions the connection between stationary solutions of such models and orbits of corresponding maps. If one considers interactions up to rth-nearest neighbors, these stationary solutions are related to the orbits obtained by iterated application of a $(2r-2)$-dimensional map. The sequence of one component of the iteration points of this map corresponds to the sequence of distances v_n between neighboring atoms. There are three important types of orbits: periodic, quasiperiodic, and chaotic. The first two represent crystalline and incommensurate states of solids, respectively. Therefore, it may be supposed that chaotic orbits can be identified with amorphous structures. This identification would give a microscopic explanation of amorphicity. In chaotic regions of maps, which we define here to be neighborhoods of transverse homoclinic points, there exist embeddings of the Bernoulli shift into the map.[14,20–22] Because of this, and the simplicity of the Bernoulli shift, we use this special map, or equivalently, the Baker transformation to generate chaotic configurations. This reduction of the original problem preserves the main features of the chaotic orbits and it allows us to derive analytical results for the pair distribution function of the corresponding configuration.

This paper is organized as follows: In Sec. II we demonstrate how the chaotic configurations are generated. The results for the jth-nearest-neighbor distribution function G_j and the pair distribution G are presented in Sec. III, and Sec. IV contains a discussion of the results. The mathematical details of the proofs of the results in Sec. III will be published elsewhere.[23]

II. CHAOTIC CONFIGURATIONS

We consider one-dimensional configurations of atoms, which are constructed in the following way: The atomic positions u_n are given by

$$u_{n+1}-u_n=v_n=A+Bx_n, \quad A>0,\ B>0 \tag{1}$$

where we fix $u_0=0$ without restriction of generality. If the mean value of the quantities x_n is zero, we have

$$\lim_{N\to\infty}\frac{1}{2N}(u_{n+N}-u_{n-N})=A \quad \text{for all } n\ . \tag{2}$$

This means that A is the mean distance of neighboring atoms. The parameter B is a measure of the deviations of the nearest-neighbor distances from their mean value A. The quantites x_n in (1) are generated by the Baker transformation, which we prefer to the Bernoulli shift, because it can be better illustrated. x_n is expressed by the transformation T by

$$x_n=(T^n(\alpha,\beta))_1-\tfrac{1}{2}\ . \tag{3}$$

Starting with an initial point (α,β), x_n is the x component of the nth iteration point of the Baker transformation, reduced by $\frac{1}{2}$. This transformation is given by

$$T\colon\ [0,1)^2\to[0,1)^2\ ,$$
$$T(x,y)=\begin{cases}(2x,\frac{1}{2}y) & \text{for } 0\le x<\frac{1}{2}\ ,\\ (2x-1,\frac{1}{2}(y+1)) & \text{for } \frac{1}{2}\le x<1\ .\end{cases} \tag{4}$$

Figure 1 illustrates the action of the Baker transformation and Fig. 2 the relationship between its orbits and the configurations.

The choice of the Baker transformation to construct chaotic structures is motivated as follows: As already mentioned in the Introduction, for models of atomic chains with interactions up to the rth nearest neighbors, there is a correspondence between the sequence of atomic distances and the sequence of points generated by iteration of a $(2r-2)$-dimensional map F. Typically, such a nonlinear map will have regions with chaotic orbits. A general feature of such a region is that there exists an embedding of the Bernoulli shift or the Baker transformation into the map.[20,21] This means that in this region the map F is a deformation of the Baker transformation in the following sense: There exists an F-invariant set $A\subset\mathbb{R}^{2r-2}$ and a transformation φ: $A\to[0,1)^2$, such that

$$F\mid_A=\varphi^{-1}\circ T\circ\varphi\ . \tag{5}$$

This implies that the iteration points of F restricted to A and the iteration points of T are connected by the transformation φ, which is independent of the iteration index n. Instead of starting from a special potential, which would lead to a special map F, it is therefore natural to take the Baker transformation, which unifies the characteristic features of chaotic regions of such maps, and to look at the properties of configurations generated by this map.

The presence of short-range order in an amorphous structure is reflected in our configurations by the strong correlations of successive v_n, which are bounded between $A-\frac{1}{2}B$ and $A+\frac{1}{2}B$, which is obvious from (1) and (3). The fact that these correlations, which depend on B/A, decay exponentially,, and that the deviations of the jth nearest-neighbor distances from their mean value jA increase with j, is also consistent with the absence of long-range order in amorphous solids. The ratio B/A is the crucial parameter in our configuration; it is a measure of short-range order. We assume $0<B/A<2$ to ensure $v_n>0$.

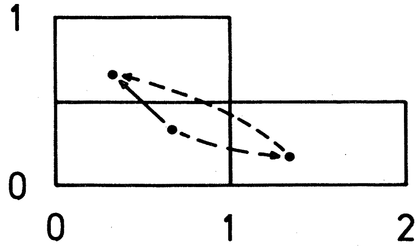

FIG. 1. Action of the Baker transformation: The unit square is first deformed to be twice as large in length and half as large in width, then the right-half part of the obtained rectangle is shifted to the top of the left part to get a map from the unit square to itself.

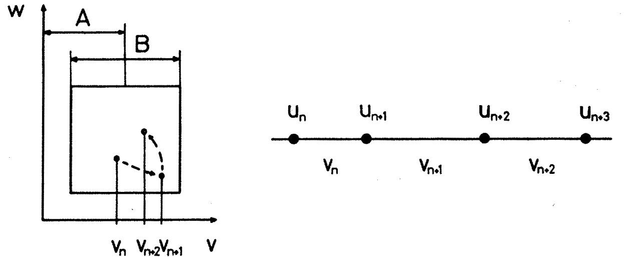

FIG. 2. Correspondence of the x component of the orbit of the Baker transformation (within the square of length B) to the atomic distances of the configuration.

III. PAIR DISTRIBUTION FUNCTIONS

To decide whether the chaotic configurations of Sec. II can represent the atomic arrangement of amorphous structures, we examine the following distribution functions: G_j, the distribution function for the jth-nearest-neighbor distances and G, the pair distribution function of the configuration. These functions are related to each other by

$$G=\sum_{j=1}^{\infty} G_j \ . \tag{6}$$

G_j can be determined as follows. The jth-nearest-neighbor distances are given by

$$u_{n+j}-u_n=D_j((T^n(\alpha,\beta))_1) \ , \tag{7}$$

where D_j is the function

$$D_j\colon \ [0,1)\rightarrow \mathbb{R}^+$$

defined by

$$D_j(x)=jA+B\sum_{l=0}^{j-1}\{[2^l x \pmod 1)]-\tfrac{1}{2}\} \ . \tag{8}$$

Because the x components of the iteration points are uniformly distributed in the unit interval for α and β normal numbers (this is obvious from the definition of normal numbers; see Niven[24]), i.e., with density $p(x)=1$, we have to calculate the distribution of $D_j(x)$ with the assumption $p(x)=1$. Let $N_j(R)$ be the number of solutions $x_\nu(R)\in[0,1)$ of

$$D_j(x)=R \ . \tag{9}$$

The probability that the jth-nearest-neighbor distance is between R and $R+dR$ is by definition $A^{-1}G_j(R)dR$, which is given by

$$A^{-1}G_j(R)dR=\sum_{\nu=1}^{N_j(R)} p(x_\nu(R))\,|dx_\nu| \ , \tag{10}$$

where dR and dx_ν are related by

$$\left.\frac{dD_j}{dx}\right|_{x=x_\nu} dx_\nu=dR \ . \tag{11}$$

Using $p(x)=1$ and

$$\frac{dD_j}{dx}(x)=B\sum_{l=0}^{j-1}2^l=B(2^j-1)$$

almost everywhere, it follows from Eqs. (10) and (11) that

$$G_j(R)=\frac{AN_j(R)}{B(2^j-1)} \ . \tag{12}$$

The mean atomic distance A is introduced in Eqs. (10) and (12) in order to make G_j dimensionless.

Hence, G_j is a piecewise constant function, which is zero outside the interval $[j(A-\tfrac{1}{2}B),\ j(A+\tfrac{1}{2}B)]$. For small j, G_j can easily be calculated according to Eq. (12). Figure 3 shows the behavior of G_j for some values of j and in Fig. 4, G_1-G_{12} are represented in the same scale to display their relative positions and heights. For large j, this procedure becomes laborious because the number of steps of G_j grows exponentially with j. But for the asymptotic behavior of G_j for $j\rightarrow\infty$ an explicit expression can be derived.

For convenience we define

$$Y_j(x)=\frac{1}{B}[D_j(x)-jA] \ . \tag{13}$$

Then the number of solutions of Eq. (9) is of course equal to the number of solutions of

$$Y_j(x)=\frac{1}{B}(R-jA) \ . \tag{14}$$

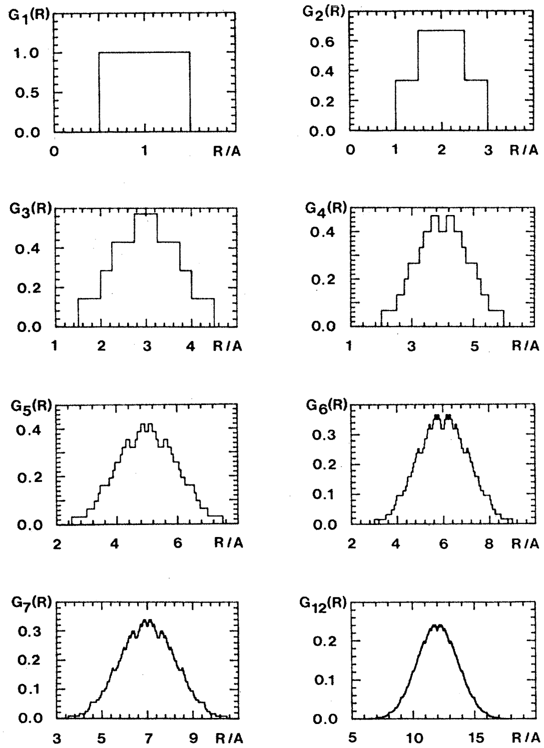

FIG. 3. Behavior of the distribution functions G_j for $B/A=1$ and some values of j. The essential form of G_j is independent of the parameter value; B/A only determines its width.

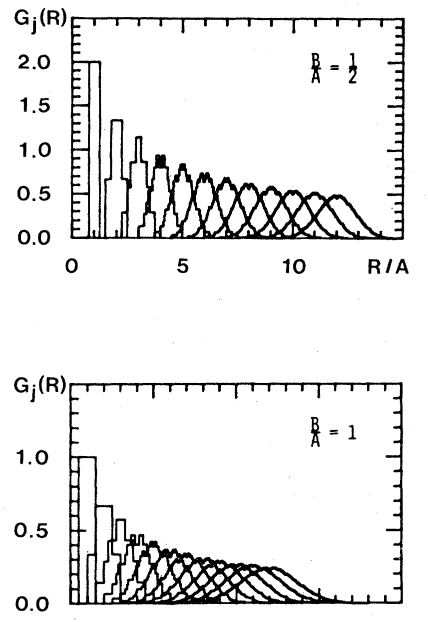

FIG. 4. Distribution functions G_1–G_{12}, visualizing the overlap of the G_j's for two different values of A/B.

The function Y_j can be split into two parts:

$$Y_j(x)=Y_j^1(x)+Y_j^2(x)\ ,$$

$$Y_j^1(x)=-\frac{k}{2^{j-1}}-\frac{1}{2}+\left[2-\frac{1}{2^{j-1}}\right]\Delta x\ , \tag{15}$$

$$Y_j^2(x)=\sum_{\nu=0}^{j-2}\sigma_\nu(k)-\frac{j-1}{2}$$

with

$$k=[2^{j-1}x]=\sum_{\nu=0}^{\infty}\sigma_\nu(k)2^\nu,\quad \Delta x=2^{j-1}x-k\in[0,1)\ , \tag{16}$$

where $[x]$ denotes the integer part of x and $\sigma_\nu(k)$ the binary digits of k. This decomposition reveals the structure of the function Y_j as shown in Fig. 5. The graph of Y_j^1 is a set of parallel lines of slope 2^{j-1}, which are contained in a strip of slope equal to -1. Y_j^2 spreads these lines into j strips, which are parallel to the original one. The number of lines in each strip is related to the number of sequences $\{\sigma_\nu\}_{\nu=0}^{j-2}$, for which

$$\sum_{\nu=0}^{j-2}\sigma_\nu(k)=m=\text{const}\ , \tag{17}$$

where the positive integer m depends on the strip. Because σ_ν equals 0 or 1, the number of sequences fulfilling Eq. (17) is equal to the binomial coefficient $\binom{j-1}{m}$. Therefore, the number of solutions of Eq. (13) is closely related to the binomial distribution, which, as is well known, can be approximated by the Gaussian distribution. This leads finally to the following.

Theorem 1:

$$\lim_{j\to\infty}\frac{B\sqrt{j}}{2A}G_j\left[jA+\frac{B\sqrt{j}}{2}\right]=\frac{1}{\sqrt{2\pi}}\exp\left[-\frac{z^2}{2}\right] \tag{18}$$

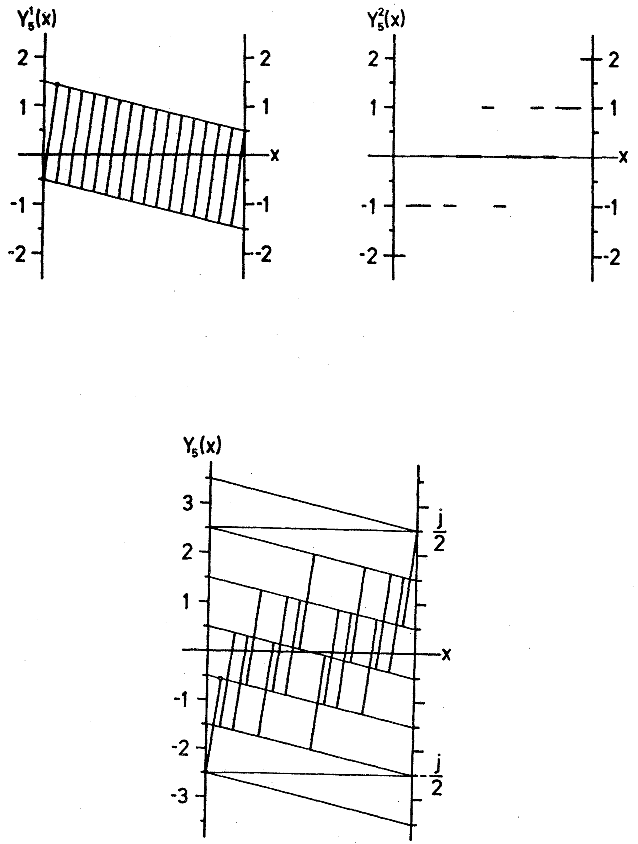

FIG. 5. Decomposition of $Y_5=Y_5^1+Y_5^2$ according to formula (15).

for all $z\in\mathbb{R}$, uniformly in every bounded z interval.

This theorem states that the distribution function of jth nearest-neighbor distances G_j behaves asymptotically as a Gaussian distribution, which is centered at jA and the width of which grows as $\sqrt{j}$. The details of the proof which is based on the ideas described above, and the equivalence of the theorem with a local-limit theorem of strongly dependent random variables, are given in Ref. 23.

The pair distribution function G can be calculated according to formulas (6) and (12). For fixed R, the sum of formula (6) consists only of a finite number of nonzero terms, because G_j is zero outside $[j(A-\frac{1}{2}B),\ j(A+\frac{1}{2}B)]$:

$$G(R)=\sum_{j=\left[\frac{2R}{2A+B}\right]}^{\left[\frac{2R}{2A-B}\right]}G_j(R)\ . \tag{19}$$

Therefore, for small R, only a few G_j contribute to G. Figure 6 shows the pair distribution function G for $0\le R\le 5A$ and three different ratios B/A.

In order to determine the asymptotic behavior of G for $R\to\infty$, the following approach is useful: For large enough j, we approximate G_j by a Gaussian distribution with standard deviation $\sigma_j=\frac{1}{2}B\sqrt{j}$ (Theorem 1). Then G, which is the sum over the G_j's, is approximated by a sum of Gaussian distributions, which are centered at the positions jA. The main contribution to this sum originates in a range of j value with size of the order of $\sqrt{j_R}$ around $j_R=[R/A]$. Within this range, the dependence of the width of the distributions on j can be neglected, and our sum can be reinterpreted to a sum over values and one Gaussian distribution, taken at points which are separated by A. Because the width of this single distribution grows as $\sqrt{j_R}$, this sum tends in the limit of large R to A^{-1} times the integral of the distribution, which is, according to our normalization, equal to A. Thus we conclude as follows.

Theorem 2:

$$\lim_{R\to\infty} G(R)=1\ . \tag{20}$$

The proof of this theorem can also be found in Ref. 23. We remark that this convergence to 1 is a necessary condition for amorphicity and reflects the absence of long-range order.

IV. DISCUSSION

The pair distribution function of our configurations generated by the Baker transformation resembles that of an amorphous solid: On one hand it exhibits the absence of long-range order due to the property that $G(R)\to 1$ for $R\to\infty$ (Theorem 2), which by itself is based upon the fact that the deviation of the jth-nearest-neighbor distances from their mean value jA is proportional to $\sqrt{j}$. On the other hand, they show the short-range order, which depends sensitively on B/A. For decreasing B/A, more and more peaks appear in G. Thus to resemble the pair distribution function of an amorphous solid, where only nearest-, next-nearest-, third-, fourth-, and perhaps fifth-nearest-neighbor peaks appear, B/A has to be fairly large. This leads to the peculiarity that the first peak of G can originate from a superposition of nearest and next-nearest neighbors (compare Figs. 4 and 6 with $B/A=1$). In three-dimensional systems, B/A can be much smaller (see Polk[2]), such that this peculiarity need not be present.

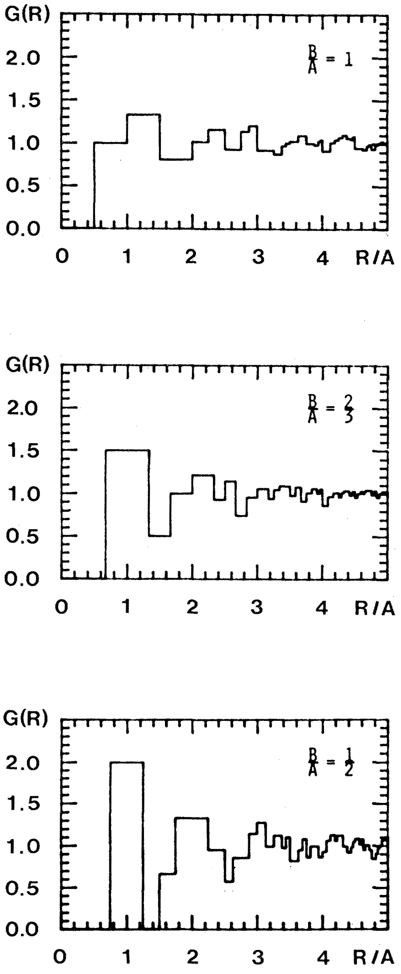

FIG. 6. Pair distribution function of our chaotic configurations for three different values of the parameter B/A.

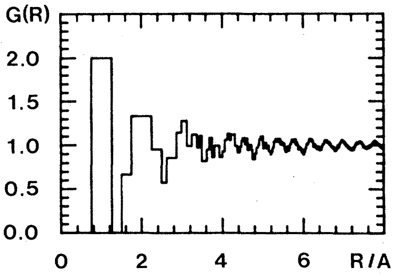

FIG. 7. Pair distribution function for $B/A=\frac{1}{2}$ for a larger range of R values.

After these first peaks, the pair distribution function shows an oscillatory behavior with decreasing amplitude. The "period" of these oscillations is not as expected equal to A (see Fig. 7). The origin of this becomes obvious by comparing Figs. 4 and 7. The deviations of the contributing G_j's from Gaussian distributions are larger than the oscillations with period A, which would arise from Gaussian distributions. In particular, the fact that the G_j's have two central peaks leads to the absence of period A.

In conclusion, we can say that the one-dimensional chaotic configurations we have generated by the Baker transformation may be interpreted as one-dimensional amorphicity at least concerning the atomic arrangement, which is characterized by the pair distribution function. Further efforts in mainly two directions are necessary: first, the investigation of one-dimensional configurations generated by chaotic maps, which originate from an interaction potential (considering the embedding of the Bernoulli shift), and second, the generalization to higher dimensions. Mainly the last point seems to be important, because the dimensionality of space may be crucial for the phenomenon of amorphicity.

ACKNOWLEDGMENTS

We would like to thank H. Thomas for bringing the problem to our attention and for carefully reading the manuscript, and P. Taklner for valuable remarks. This work was supported in part by the Swiss National Science Foundation.

[1] W. H. Zachariasen, J. Am. Chem. Soc. 54, 3841 (1932).

[2] D. E. Polk, J. Non-Cryst. Solids 5, 365 (1971).

[3] D. E. Polk and D. S. Boudreaux, Phys. Rev. Lett. 31, 92 (1973).

[4] R. Dandoloff, G. Döhler, and H. Bilz, J. Non-Cryst. Solids 35 and 36, 537 (1980).

[5] G. Döhler, R. Dandoloff, and H. Bilz, J. Non-Cryst. Solids 42, 87 (1980).

[6] C. H. Bennett, J. Appl. Phys. 43, 2727 (1972).

[7] K. Maeda and S. Takeuchi, J. Phys. F 8, L283 (1978).

[8] J. L. Finney, Proc. R. Soc. London, Ser. A 319, 479 (1970).

[9] N. Rivier and D. M. Duffy, J. Phys. (Paris) 43, 293 (1982).

[10] N. Rivier, Philos. Mag. A 45, 1081 (1982).

[11] M. Kléman and J. F. Sadoc, J. Phys. (Paris) Lett. 40, L569 (1979).

[12] J. F. Sadoc, J. Non-Cryst. Solids 44, 1 (1981).

[13] V. I. Arnold and A. Avez, *Ergodic Problems in Classical Mechanics* (Benjamin, New York, 1968).

[14] J. Moser, *Stable and Random Motions in Dynamical Systems* (Princeton University Press, Princeton, N.J., 1973).

[15] P. Collet and J.-P. Eckmann, *Iterated Maps on the Interval as Dynamical Systems* (Birkhäuser, Basel, 1980).

[16] S. Aubry, in *Stochastic Behavior in Classical and Quantum Hamiltonian Systems,* Vol. 93 of *Lecture Notes in Physics,* edited by G. Casati and J. Ford (Springer, New York, 1979).

[17] D. Ruelle, Physica (Utrecht) 113A, 619 (1982).

[18] S. Aubry, in *Solitons and Condensed Matter Physics,* edited by A. R. Bishop and T. Schneider (Springer, New York, 1979).

[19] T. Janssen and A. Tjon, J. Phys. A 16, 673 (1983).

[20] S. Smale, in *Differential and Combinatorial Topology,* edited by S. Cairns (Princeton University Press, Princeton, N.J., 1965).

[21] S. Smale, Bull. Am. Math. Soc. 73, 747 (1967).

[22] C. C. Conley, in *Dynamical Systems, Theory, and Applications,* Vol. 38 of *Lecture Notes in Physics,* edited by J. Moser (Springer, New York, 1975).

[23] P. Reichert and R. Schilling (unpublished).

[24] I. Niven, *Irrational Numbers, The Carus Mathematical Monographs II* (Wiley, New York, 1956).